NeuroImage 256 (2022) 119247

Contents lists available at ScienceDirect

NeuroImage

journal homepage: www.elsevier.com/locate/neuroimage

Power shift and connectivity changes in healthy aging during resting-state EEG

Alessio Perinelli[#,*], Sara Assecondi, Chiara F. Tagliabue, Veronica Mazza

Center for Mind/Brain Sciences (CIMeC), University of Trento, Corso Bettini 31, 38068 Rovereto, TN, Italy

ARTICLE INFO

Keywords:
EEG
Resting-state
Connectivity
Aging

ABSTRACT

The neural activity of human brain changes in healthy individuals during aging. The most frequent variation in patterns of neural activity are a shift from posterior to anterior areas and a reduced asymmetry between hemispheres. These patterns are typically observed during task execution and by using functional magnetic resonance imaging data. In the present study we investigated whether analogous effects can also be detected during rest and by means of source-space time series reconstructed from electroencephalographic recordings. By analyzing oscillatory power distribution across the brain we indeed found a shift from posterior to anterior areas in older adults. We additionally examined this shift by evaluating connectivity and its changes with age. The findings indicated that inter-area connections among frontal, parietal and temporal areas were strengthened in older individuals. A more complex pattern was shown in intra-area connections, where age-related activity was enhanced in parietal and temporal areas, and reduced in frontal areas. Finally, the resulting network exhibits a loss of modularity with age. Overall, the results extend to resting-state condition the evidence of an age-related shift of brain activity from posterior to anterior areas, thus suggesting that this shift is a general feature of the aging brain rather than being task-specific. In addition, the connectivity results provide new information on the reorganization of resting-state brain activity in aging.

1. Introduction

Healthy aging is associated with an average decline of cognitive performance (Fabiani, 2012; Hedden and Gabrieli, 2004), which in turn correlates with changes in brain activation patterns (Eyler et al., 2011; Grady, 2012, Salallonch et al., 2015). Significant work has quantified the effects of cognitive healthy aging in terms of neurophysiological signals: after seminal studies relying on positron emission tomography (PET) (Grady et al., 1994; Reuter-Lorenz et al., 2000; Cabeza et al., 1997), extensive research has investigated aging effects on neuronal activity, exploiting functional magnetic resonance imaging (fMRI) (Cabral et al., 2017; Hrybouski et al., 2021; Escrichs et al., 2021) (see Sugiura (2016) for a recent review) and, less frequently, electroencephalography (EEG) (Knyazev et al., 2015; Fleck et al., 2017) and magnetoencephalography (MEG) (Tibon et al., 2021).

Often reported in the literature is an increased prefrontal activity in older adults during task execution (Festini et al., 2018; Turner and Spreng, 2012; but see Grady, 2012 and Salallonch et al., 2015). Several models have been proposed to explain the age-related prefrontal overactivation. For example, the hemispheric asymmetry reduction in older adults (HAROLD) model (Cabeza, 2002) hypothesizes that, when executing a given cognitive task, the activation of prefrontal areas is less lateralized (more bilateral) in older adults with respect to young individuals (Cabeza, 2002; Learmonth et al., 2017). Indeed, experimental evidence from fMRI and PET studies on older adults showed more homogeneous activity across hemispheres during tasks that involved several different high-level cognitive functions, such as episodic memory retrieval, working memory, perception and inhibitory control (see Dolcos et al., 2002 for a review).

The posterior-anterior shift in aging (PASA) model (Davis et al., 2008; Dennis and Cabeza, 2008), predicts decreased activation of posterior areas and concurrent increased activation of anterior areas in older adults compared to young controls. The model suggests that the frontal over-engagement occurs in response to an age-related decline in functional integrity of posterior regions (Davis et al., 2008). The PASA account is supported by observations in several cognitive domains (e.g., visual attention, working memory, episodic memory) thus suggesting that the posterior-to-anterior shift is not restricted to a specific cognitive function (Festini et al., 2018), and potentially also affects activity at rest. Indeed, some evidence of a PASA-like effect in resting-state fMRI exists (McCarthy et al., 2014; Ren et al., 2019), suggesting that the mechanism underlying the posterior-to-anterior shift can be closely linked not

* Corresponding author.
E-mail address: alessio.perinelli@unitn.it (A. Perinelli).
Present address: Department of Physics, University of Trento – Via Sommarive 14, 38123 Trento, Italy

https://doi.org/10.1016/j.neuroimage.2022.119247.
Received 26 November 2021; Received in revised form 20 April 2022; Accepted 23 April 2022
Available online 25 April 2022.

only to functional (i.e., task-related), but also to structural changes in the aging brain.

Several studies have provided support to the HAROLD and PASA models (Schneider-Garces et al., 2010; Cabeza and Dennis, 2012; Ansado et al., 2012; Li et al., 2015; Tagliabue et al., 2022). Nonetheless, a thorough understanding of the mechanisms underlying higher frontal activations in older adults is lacking (Eyler et al., 2011; Morcom and Johnson, 2015). In particular, it is not clear whether the increase in activity in anterior areas is due to increased activity within those areas or to a higher engagement of those areas in a network, i.e. an increased connectivity between regions. In support to the latter hypothesis, an increased connectivity between different functional networks was indeed detected in older adults during the execution of different tasks (Rieck et al., 2021; Geerligs et al., 2014; Chan et al., 2014).

In light of these issues, the goal of the present study is to investigate whether the age-related changes predicted by PASA and HAROLD accounts can be verified by leveraging the use of resting-state electrophysiological (EEG) recordings and of connectivity measures.

Most literature, as well as related theoretical models, focuses on task-related changes. Observed changes are, thus, interpreted by considering the cognitive function engaged by the task and the performance outcome. Nevertheless, some studies have investigated the effects of age on brain activation at rest and found a general age-related decreased activity in specific resting-state networks (Andrews-Hanna et al., 2007; Damoiseaux et al., 2008; Geerligs et al., 2015; Song et al., 2014; Balsters et al., 2013), as well as less distinct functional separation between those networks (Geerligs et al., 2015; Song et al., 2014). Resting-state measurements have the advantage of probing neural activity that is independent of any specific task, and thus allow researchers to test more general assumptions concerning age-induced changes of brain activation. As the PASA and HAROLD models are supported by observations covering many cognitive domains, the models should, in principle, reflect general effects of aging on brain activity. Therefore, the age-related anterior shift and/or reduced lateralization of neural activity should be detected even during a condition of wakeful rest.

The models mentioned above were developed by relying heavily on fMRI observations. However, the blood-oxygen-level-dependent (BOLD) signal probed by fMRI is an indirect measure of neural activity and, because it depends on vascular topography, it might be affected by age-related alterations of the cerebral vascular structure, leading to spurious connectivity assessments (D'Esposito et al., 2003; Hillary and Biswal, 2007). Additionally, fMRI has a low temporal resolution, which does not enable a detailed view of the time course of brain activity. In contrast, EEG and MEG are direct measures of neural activity, and have a higher temporal resolution than fMRI. Indeed, EEG/MEG time series analysis techniques, such as entropy-related (Shumbayawonda et al., 2017; Mcintosh et al., 2014) and connectivity (Bowyer, 2016; Crouch et al., 2018; Bastos and Schoffelen, 2016) measures can provide a more accurate picture of the dynamics of communication within brain regions with respect to BOLD signals, which are limited by the slow temporal fluctuations of the hemodynamic response (Rossini et al., 2019).

Some EEG and MEG studies have investigated age-related changes in power and frequency content. For example, a recent MEG study (Tibon et al., 2021) analyzed fast (below 1 second) transient dynamics of resting-state networks and showed that such dynamics depend on age. In this framework, an age-related decrease in slow-wave power has been repeatedly found across the whole scalp, both at rest and during task execution (Vlahou et al., 2014, Cummins and Finnigan, 2007, Leirer et al., 2011). The analysis of power provides information analogous to the one extracted from fMRI: indeed, as a rough approximation, fMRI activations can be considered proportional to local neural activity (Heeger and Ress, 2002; Logothetis et al., 2001), and thus, on average, to EEG power. However, the mechanisms underlying power alteration patterns in aging remain unknown (Tatti et al., 2016; Finnigan and Robertson, 2011). Specifically, power measures do not allow for a distinction between intra-area versus inter-area changes in neural activity. Functional connectivity provides exactly this information.

Several measures are used to estimate connectivity. Here we focus on two methods: the "Cross-correlation Time scale of Observability" (CTO) (Perinelli et al., 2018) and mutual information (MI) (Cover and Thomas, 2006). The CTO method is based on the evaluation of running-window cross-correlations, whose statistical significance is assessed via surrogate-based estimation, a data-driven method to construct null-hypothesis distributions (Schreiber and Schmitz, 2000). By virtue of these two key elements, this method deals well with non-stationary and non-linear signals, as in the case of resting-state electrophysiological signals (Perinelli et al., 2018). Moreover, given the algorithm implemented in the surrogate generation step, CTO is also robust against spurious correlations solely due to the long-range autocorrelation that might characterize the data (Perinelli et al., 2021). The CTO method has been previously used to identify and characterize brain networks out of MEG recordings, showing for example that the time scale of observability of a link depends, on average, on the logarithm of the physical distance between the nodes (Perinelli et al., 2019; Castelluzzo et al., 2021).

Mutual information (MI) is a metric that quantifies statistical dependence between two distributions by relying on the information-theoretical concept of entropy (Cover and Thomas, 2006). Due to its generality and its straightforward interpretation as a measure of connectivity strength, MI has been widely used in neuroscience (Rossini et al., 2019; Quian Quiroga and Panzeri, 2009; Timme et al., 2014; Jeong et al., 2001). It was recently shown that the results of the CTO method and MI in the analysis of connectivity are consistent, and the two methods can be considered as complementary (Perinelli et al., 2021). Indeed, both methods are non-parametric and yield non-directed estimates of connectivity that are, on average, proportional. The relationship between the two, however, breaks down in the limit of strong cross-correlation, because the CTO method "saturates" to its maximum detectable connectivity. Moreover, it was shown that the CTO method is more conservative—and thus more robust—than MI in detecting weak cross-correlations (Perinelli et al., 2021). Consequently, the two methods were used here to probe two complementary connectivity regimes, namely the (strong) intra-area connectivity (MI), and the (weaker) inter-area connectivity (CTO).

The assessment of connectivity also allowed us to apply metrics from graph theory to further characterize the observed networks. A few previous EEG studies (Knyazev et al., 2015; Gaál et al., 2010; Zangrossi et al., 2021) on resting-state connectivity showed that older adults exhibit a higher amount of random connections, as reflected by changes in modularity (a graph-theoretical measure of network organization, see Sporns and Betzel, 2016, Newman, 2006). Changes in modularity are considered a biomarker of cognitive plasticity and cognitive performance (Gallen and D'Esposito, 2019). For instance, higher modularity is often associated with better performance or higher plasticity (following training) in young and older adults (Arnemann et al., 2015; Baniqued et al., 2018), while a general decrease in modularity with age has been observed (Knyazev et al., 2015; Geerligs et al., 2015; Song et al., 2014).

To investigate whether the age-related changes predicted by PASA and HAROLD accounts can be verified by means of EEG and in the absence of any task, here we analyzed the "Leipzig Study for Mind-Body-Emotion Interactions" (LEMON) public database (Babayan et al., 2019), which contains EEG resting-state recordings of both young and older adults. The use of resting-state recordings allowed us to test models of neurocognitive aging in a more general framework, independently of any specific task. We chose to focus on the PASA and HAROLD models, as they provide specific indication on how spatial activation patterns are modulated by age. To evaluate the relative contribution of intra- and inter-area neural changes related to aging, and in addition to the more traditional measures of power, we focused on connectivity measures and we further characterized brain networks using a modularity index. While EEG and MEG studies of age-related changes in power and

frequency content are often limited to analysis in sensor-space, here we reconstructed time series of brain activity in source space. This allowed us to achieve a more accurate assessment of correlations between brain activations (Van de Steen et al., 2019; Brunner et al., 2016).

We expected significant differences in power distributions between age groups either along the posterior-anterior direction (i.e. more power in frontal areas of older adults) or across hemispheres (i.e. reduced asymmetry of power distribution for older adults), corresponding to the predictions of the PASA and HAROLD models, respectively. In addition, as stated above, we expected the MI and CTO measures to provide additional, crucial information on the contribution of intra-area (MI) and inter-area (CTO) connectivity to the resulting (if present) anterior overactivation in older adults. Consistently with previous works (Knyazev et al., 2015; Geerligs et al., 2015; Song et al., 2014), we expected that changes in network structure highlighted by the connectivity analysis would also be characterized by a lower modularity, i.e. a "less segregated" network arrangement (Gallen and D'Esposito, 2019), in older with respect to young adults.

The dataset analyzed in the present study contains resting-state recordings in two conditions, namely eyes-closed (EC) and eyes-open (EO). Previous EEG resting-state studies showed that brain activity is overall reduced in EO with respect to EC, although this difference is not modulated by age (Barry and De Blasio, 2017; Stacey et al., 2021). Therefore, we did not expect differences between the two conditions in the two age groups. In addition, while the HAROLD and PASA models have specific hypotheses on an age-related reorganization of brain activity, they have been developed and tested on task-evoked activity; therefore, they do not allow for differential hypotheses between EO and EC conditions. Nonetheless, to allow for a more general and thorough investigation, we decided to analyze both conditions (EC/EO), without merging them together. Because of restrictions due to the methodology (see Methods), we focused the analyses on the theta, alpha, and beta bands, often considered in aging studies (Puligheddu et al., 2005; Stacey et al., 2021; Chow et al., 2022). Increased alpha band during resting-state in young adults has been related to reduced functional connectivity within visual and attentional systems, and considered as indicative of enhanced functional inhibition (Chang et al., 2013; Scheeringa et al., 2008; Tagliazucchi et al., 2012). Given the hypothesized HAROLD and PASA-related modulations of power distribution, a reduction of posterior alpha power in older adults could in turn result in higher connectivity at rest compared to younger individuals. In contrast, significantly less is known about the functional role of theta- and beta-band activity during rest (Moosmann et al., 2003; Laufs et al., 2003; Jensen et al., 2005; Scheeringa et al., 2008). For this reason, we did not make specific predictions on the functional significance of age-related changes in these two frequency bands and their investigation was mainly explorative.

2. Methods

2.1. Dataset and preprocessing

EEG recordings of 30 young (aged 25–35, 19 males, 11 females) and 30 older adults (aged 60–80, 19 males, 11 females) were selected from the LEMON public database (Babayan et al., 2019). The data recording protocol was approved by the ethics committee at the medical faculty of the University of Leipzig (reference number 154/13-ff) and was in accordance with the Declaration of Helsinki. The raw EEG session consists of a resting-state acquisition of 16 segments of interleaved eyes-closed (EC) and eyes-open (EO) (8 segments for each condition) between 60 s and 90 s long. Among them, we selected three EC and three EO segments, corresponding to the segments between the third and the eighth (both included), to discard any initial transient. The length of each segment was trimmed to 60 s by symmetrically removing data points from both ends after the preprocessing stages. EEG signals were recorded via a 62-channels ActiCAP with active electrodes, with standard 10–20 placement (Oostenveld and Praamstra, 2001) and sampled through a BrainAmp MR plus amplifier in an electrically shielded and sound-attenuated room. Raw recordings were bandpass-filtered between 0.015 Hz and 1 kHz and sampled at a 2.5 kHz rate. Details on data acquisition protocol are provided in Babayan et al. (2019).

Preprocessing of raw EEG data was carried out by means of custom MATLAB code relying on routines provided within the FieldTrip toolbox (Oostenveld et al., 2011). Resting-state recordings are characterized by a lower signal-to-noise ratio compared to task-evoked data, also due to the fact that averaging of multiple trials is impossible. Noise contamination due to muscular activity and saccades, which typically affects the high-frequency part of the spectrum (Muthukumaraswamy, 2013; Yuval-Greenberg et al., 2008), might be spuriously identified as of neural origin (Pope et al., 2009). For these reasons, as typically done in resting-state EEG, we filtered the data with a low-pass filter at 40 Hz (Michel and Brunet, 2019), at the cost of excluding the gamma band from our analysis. The exclusion of the delta band, on the other hand, stems from time scale issues as discussed in Section 2.3. Besides a 40 Hz low-pass filter, recordings were filtered through a 0.1 Hz high-pass filter and a 50 Hz notch filter (2 Hz width). All filters were implemented as fourth-order Butterworth two-pass filters. The notch filter is required because of the insufficient attenuation of the 50 Hz line noise provided by the low-pass filter (approximately 0.15, or −16 dB). Upon filtering, data were down-sampled to a 250 Hz sampling rate. Poor quality channels, labeled as such in the original dataset, were interpolated (spherical spline interpolation of neighboring channels). To remove cardiac, muscular and eye-movement artifacts, an independent component analysis was carried out by running the "fastica" algorithm available in FieldTrip: the temporal features and spatial topology of the resulting components were visually examined to reject artifactual ones. Each subject's recording was bandpass-filtered in three frequency bands ([4 Hz, 8 Hz] (theta band), [8 Hz, 14 Hz] (alpha band), and [14 Hz, 30 Hz] (beta band), obtaining three time series for each subject. These time-series were then reconstructed in source space as described in the following section.

The choice of the boundaries of the three bands complies with standard frequency values that are commonly considered in the literature to define the three bands (Balsters et al., 2013; Scally et al., 2018; Moezzi et al., 2019). Aging is known to produce a slowing of the EEG rhythms, namely a reduction of the frequency of brain oscillations, although the functional meaning of each band is assumed to remain the same, irrespective of age (Chiang et al., 2011; Scally et al., 2018). As far as the present analysis is concerned, the potential age-related slowing of rhythms is not expected to significantly change our results. Indeed, the analysis does not rely on the frequency or amplitude of spectral peaks, but rather on time series filtered within the whole band. By virtue of the time-domain (rather than frequency-domain) connectivity methods that were considered here (see "Power and connectivity analysis" below), a shift in rhythm frequency would not significantly alter the connectivity estimates, provided that the driving frequency of the oscillation is still contained within the band limits. Nevertheless, to ensure that the band frequency limits selected here were reliable for both age groups we estimated the individual theta, alpha and beta peak frequency of each participant, and evaluated whether each frequency peak belonged to the respective band limits as defined here. Details concerning this validation procedure, as well as the related results, are reported in the Supplementary Materials. The results show that all participants' peak frequencies fell within the respective band limits (Supplementary Materials, Figure S4).

2.2. Source reconstruction

Source reconstruction was carried out by exploiting the individual preprocessed anatomical MRI scans that are available within the LEMON database. For each subject, an individual head model was generated by segmenting the anatomical MRI to provide scalp, skull and brain meshes. Thereupon, a source model consisting of current dipoles was built through a nonlinear inverse-warp of a template 10 mm-resolution

grid (3294 vertices, MNI coordinates system) onto the subject brain mesh. Dipole orientations were set as unconstrained. Upon manual alignment of sensor positions onto the individual head mesh and, subsequently, their projection onto the scalp, a forward model was computed. The reconstruction of current dipoles was performed via the exact low-resolution electromagnetic tomography algorithm ("eLoreta") (Pascual-Marqui et al., 2011).

Of the 3294 vertices included in the source model, we selected 24 nodes, following the reference atlas by Glasser et al. (2016). Within each of four brain areas (occipital, parietal, temporal, and frontal) three regions were selected: V1, V6A, V4 for occipital; Pfm, PF, STV for parietal; STGa, TE1a, TA2, for temporal, and 10d, 10pp, p10p for frontal. Each region was selected both in the left and in the right hemisphere, thus yielding a total of 24 regions. The closest (lowest Euclidean distance) vertex of the source model to the centroid of each region was chosen as the node representing that region, and the time series of the source current dipole amplitude, reconstructed at that node, was extracted. The whole procedure was repeated for the three frequency bands (theta, alpha, beta) and for the two conditions (EC, EO): each band-condition combination yielded three time series, corresponding to the three segments selected from the preprocessed recordings (see above), therefore giving a total of 18 time series for each subject. These time series in source space were used as starting point to extract power density distributions and connectivity patterns.

2.3. Power and connectivity analysis

2.3.1. Area-related power

To investigate differences in power distribution across the brain between young and older adults, we extracted the power spectral density (PSD) associated to a given area as follows. For each node—for a given subject, condition, and frequency band—we calculated the average PSD estimated on the three available segments. The sum of the power values corresponding to the three nodes belonging to a given area were normalized with respect to the total power in all nodes. In this way, any multiplicative bias affecting power due to imprecise source reconstruction was ruled out.

2.3.2. Network connectivity

To investigate network dynamics underlying differences in power distribution between young and older adults, we estimated source-space connectivity using two different methods, namely the CTO method and MI. While the CTO method is used to evaluate inter-area connectivity, MI is applied to estimate intra-area connectivity. This choice stems from the observation that the CTO method is better suited in a "weak" connectivity regime, such as the one characterizing inter-area links, for which MI yields small values that are comparable with the background noise. On the contrary, MI is more suited in a "strong" connectivity regime, like in the case of intra-area connectivity, for which the CTO method saturates. Data supporting this approach of using two different methods for two different connectivity regimes, are presented in the Supplementary Materials.

2.3.3. CTO method

Fig. 1 schematically shows the main steps of the CTO method (detailed descriptions of the method are provided in Perinelli et al. (2018), Perinelli & Ricci (2019), Perinelli et al. (2021)), which consist of: 1) calculation of a cross-correlation diagram; 2) estimation of p-values associated to each element of the cross-correlation diagram via surrogate generation; 3) calculation of the efficiency function; 4) assessment of the time scale of observability W.

1 *Calculation of a cross-correlation diagram.* Given two time series, Pearson cross-correlation coefficients $r(w,k)$ are computed over running windows of width w at position k along the time series. The window width w is an integer multiple of a "base" window $w_0 = 0.08$s up to a maximum width $w_{\max} = 10$s, yielding a matrix of 125×626 elements. The two parameters w_0, $w_{\max}$ are chosen according to the sampling period and length of the available time series, respectively. Specifically, w_0 should be at least about one order of magnitude larger than the sampling period (here equal to 0.004 s), to have enough data points to compute cross-correlation coefficients (Perinelli et al., 2018). On the other hand, $w_{\max}$ should be smaller than the length of the time series (here equal to 60 s), but large enough to cover the time scale of interest. The choice of w_0 has consequences on the frequencies that can be reliably analyzed by the CTO method. Specifically, the frequency components that contribute to a given cross-correlation coefficient are those at frequencies that are integer multiples of $1/w$ (Perinelli et al., 2018): while high-frequency components essentially contribute for all values of w lower frequencies require larger windows to be correctly probed. For instance, all windows having width less than 0.5 s would not include any component from signals at 2 Hz and below (a significant part of the delta band), and the corresponding correlation coefficient would be a biased representation of that frequency band. The effect is more critical for the edge of the delta band: signals at 1 Hz would only be probed at w larger than 1 s, and signals at 0.1 Hz would not be probed for *any* w considered here. For this reason, in the present analysis we decided to exclude the delta band.

2 *Estimation of p-values associated to each element of the cross-correlation diagram.* The significance of each element of the cross-correlation diagram is assessed through a surrogate-based significance estimation (Schreiber and Schmitz, 2000; Theiler et al., 1992). Surrogate time series share specific statistical properties with the generating, "original" one, but are otherwise stochastic, and allow for data-driven estimations of unknown null-hypothesis distributions. For each one of the two sequences under analysis, $M = 200$ surrogate sequences were generated via the iterative amplitude-adjusted Fourier transform algorithm (Schreiber and Schmitz, 1996), which preserves the amplitude distribution and the power spectrum (and, consequently, the autocorrelation) of the given original sequence but not its time-correlation. For each pair of surrogate sequences, a surrogate cross-correlation diagram $r_i(w,k)$ is computed ($i = 1, M$). Given w and k, the rank of the element $r(w,k)$ of the "original" diagram among the M elements of the surrogate diagrams sorted in descending order provides, once divided by M, the related p-value. By repeating this evaluation over all w and k, a p-value diagram $p(w,k)$ of 125×626 elements is obtained, where each element represents the significance of the correlation of the original time series at position k for a window of width w.

3 *Calculation of the efficiency function.* The information contained in a p-value diagram is then further condensed by computing the efficiency function $\eta(w)$. Considering a significance threshold for p-values at 0.05, the efficiency $\eta(w)$ is defined, at a given window width w, as the fraction of elements of $p(w,k)$ larger than 0.05, that is the elements that detect a significant cross-correlation between the two original time series. The efficiency $\eta(w)$ is bounded between 0 and 1: the larger the efficiency, the higher the probability that, given a window width w, a significant cross-correlation is observed at a given point along the two corresponding time series. In other words, $\eta(w)$ quantifies how efficient is a given window width w in detecting cross-correlation between a pair of time series. In the present work, before evaluating the efficiency of a given pair of nodes, the three p-value diagrams derived from the three segments available for each band and condition (see above) were concatenated to provide a single efficiency function that condenses the information from all the three segments.

4 *Assessment of the time scale of observability W from the efficiency function $\eta(w)$.* Given an efficiency threshold η^*, W is defined as the minimum window width w, if any, for which $\eta(w) \geqslant \eta^*$. Here, η^* was set to 0.5. A detailed discussion on the role of this parameter is reported in Perinelli et al. (2021). The time scale of observability W of a link

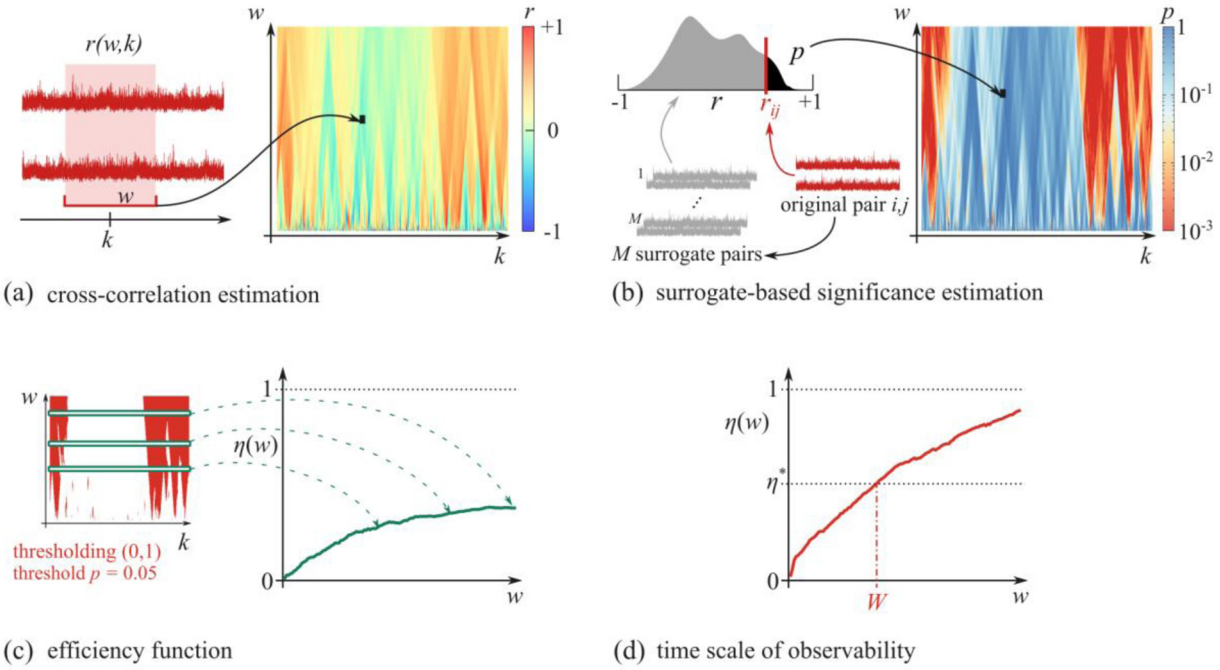

Fig. 1. Schematic diagram representing the main steps of the CTO method. (a) Calculation of a cross-correlation diagram out of a pair of time series. (b) Estimation of a p-value for each element of the cross-correlation diagram by means of surrogate generation: the M surrogate pairs of time series allow to estimate a null-hypothesis distribution of the correlation coefficient r (in gray), so that the original cross-correlation coefficient can be associated to a p-value. (c) Evaluation of the efficiency function by thresholding the p-value diagram obtained in (b) and by considering the fraction of above-threshold elements of the diagram at a given window width w. (d) Assessment of the time scale of observability W out of the efficiency function as the window width at which efficiency overcomes a threshold η^*.

between two time series is inversely proportional to the strength of the link (the larger W, the longer the time window necessary to detect a significant correlation for at least a fraction η^* of the time axis). To provide a "more natural" interpretation of the results of the CTO method, we linearly remapped the values of W into a dimensionless "connectivity strength coefficient" c by means of the following expression: $c = (w_{\max} + w_0 - W)/w_{\max}$. In this way, the strongest detectable connectivity, namely $W = w_0$, corresponds to $c = 1$; larger values of W correspond to smaller values of c, i.e. to weaker links. Finally, for the sake of consistency, a value $c = 0$ is assigned to those links for which W does not exist (i.e. links for which no connectivity is detected by the CTO method, as the efficiency never reaches the threshold η^*).

2.3.4. Mutual information

MI was calculated by relying on the Kozachenko–Leonenko k-nearest-neighbor entropy estimator (Kozachenko and Leonenko, 1987), that provides more accurate results with respect to a standard "plug-in" estimator based on histograms (Perinelli et al., 2021; Lombardi and Pant, 2016). Given two time series x, y, their Mutual information (MI) is computed as $MI(x, y) = H(x) + H(y) - H(x, y)$, where the marginal entropies $H(x)$, $H(y)$ as well as the joint entropy $H(x, y)$ are estimated through the Kozachenko–Leonenko method (the implementation used here is described in Perinelli et al. (2021)), where the number of nearest-neighbors to be considered in the evaluation of entropies was set to 20. In this case, to yield a single evaluation of MI out of the three available segments corresponding to a given band and condition, we averaged the three related MI values.

2.3.5. Area-related connectivity

Given a subject, condition, and band, the CTO method and MI both provide a single real number, c or MI, for each one of the $N = 24 \times 23/2 = 276$ available node pairs (the number of pairs is given by $m \times (m-1)/2$, where m is the number of nodes). This "fine-grained" connectivity information is necessary to compute network metrics such as modularity (see below), but redundant when considering differences between age groups. For data reduction, we calculated the area-related connectivity coefficients C_{AB} (inter-area) and MI_{AA} (intra-area) between areas as

$$C_{AB} = \frac{1}{N_{AB}} \sum_{i \in A, j \in B}^{N_{AB}} c_{ij}$$

or

$$MI_{AA} = \frac{1}{N_{AA}} \sum_{i,j \in A, i \neq j}^{N_{AA}} MI_{ij}$$

respectively, where c_{ij} is the connectivity coefficient between nodes i and j, and N_{AB} is the number of node pairs between areas A and B ($N_{AB} = 9$; in the case of intra-area connectivity, $N_{AA} = 3$). In summary, an area-connectivity coefficient is the average of the connectivity coefficients between all combinations of pair of nodes in the two areas or within the same area.

2.4. Modularity

Modularity is a graph-theoretical measure that quantifies the degree to which a network can be segregated into subnetworks, called "modules" (Newman, 2006; Gallen and D'Esposito, 2019). A high (close to 1) modularity corresponds to a network made of several, easily-distinguished groups of nodes (modules) that have many intra-module and few inter-module links. On the opposite, a randomly-connected network has vanishing modularity. For our purpose, modules were defined as sets of six nodes belonging to the same functional area. Consequently, four modules were considered, corresponding to the four selected areas (occipital, parietal, temporal, and frontal).

The computation of modularity requires a network to be defined in terms of a binary adjacency matrix (Newman and Girvan, 2004). For each participant, condition and band we built such matrix according to a procedure that combines the CTO method and MI into a single definition of the network. The combined use of CTO and MI was justified by

the fact that CTO can better detect "weaker" links as compared to MI and, consequently, CTO is suitable to assess inter-area links, while MI is more reliable in the case of intra-area links (see previous Section). The generation of the adjacency matrix was carried out as follows.

A c threshold (c_t) is first set. Then, a corresponding MI threshold (MI_t) is assessed by considering the maximum MI among all pairs of nodes for which c is lower than the threshold c_t. The c_t and MI_t thresholds are then used to binarize the connectivity matrix: an inter-area link exists if c_t, while an intra-area link exists if $MI > MI_t$. By virtue of the MI threshold evaluation, a pair that would be deemed as "not linked" according to the c_t threshold is also deemed "not linked" according to the MI threshold. This criterion is thus in compliance, on the one hand, with the fact that CTO is in general more conservative than MI (Perinelli et al., 2021) and that CTO can better detect "weaker" links as compared to MI.

Given a binary adjacency matrix representing a network, the corresponding modularity (see also Eq. 5 of Newman & Girvan (2004)) is given by

$$Q = \sum_{m=1}^{N_m} \left(e_{mm} - a_m^2\right)$$

where N_m is the number of defined modules, e_{ij} is the fraction of links in the network that connect nodes in area or module i with nodes in module j (e_{mm} is thus the number of intra-module links), and $a_i = \sum e_{ij}$ is the fraction of links connecting module i.

2.5. Statistical analysis

Statistical testing was performed via the JASP statistical software (JASP team, 2021) version 0.15. Statistically significant effects were assessed by applying a mixed ANOVA with AGE as between-subjects factor (bs) and, depending on the analysis, CONDITION, BAND, AREA and HEMISPHERE as within-subjects factors (ws). Details on each test are provided before the corresponding result is described. The compliance of dependent variables with ANOVA's assumptions (normality, homogeneity of variance) was not always met. Nevertheless, the test is sufficiently robust against departure from these assumptions to allow for its use. In particular, it was shown that for equal sample sizes (as it is the case in the present work), the heterogeneity of variances does not significantly affect the test reliability (Glass et al., 1972; Blanca et al., 2018). Similarly, it was shown that departure from normality does not affect the results of the test (Pearson, 1931; Glass et al., 1972), provided that the significance level (here set to 0.05) is not very small (e.g. 0.001). In the case of violation of sphericity, the Greenhous-Geisser correction was applied, and the corrected p-value is reported (p_{GG}). Significant effects were followed-up with post-hoc comparisons, using the false discovery rate (FDR) correction (Benjamini and Yekutieli, 2001): only adjusted p-values (p_{adj}) are reported.

3. Results

The following sections report the statistically significant results stemming from the analysis of power and connectivity. Since the focus of the study was on aging, and for the sake of clarity, below we consider only significant age-related effects. Statistical findings not related to age are reported in the Supplementary Materials.

3.1. Power

Effects on power were assessed by applying a mixed ANOVA (bs: AGE; ws: CONDITION, BAND, AREA and HEMISPHERE). The following significant effects emerged: AREA ($F_{(3174)} = 405.75$, $p_{GG} < 0.001$, $\eta^2_p = 0.88$), CONDITION ($F_{(1,58)} = 5.50$, $p = 0.023$, $\eta^2_p = 0.09$), AGE*AREA ($F_{(3174)} = 97.02$, $p_{GG} < 0.001$, $\eta^2_p = 0.63$), AREA*CONDITION ($F_{(3174)}=125.94$, $p_{GG} < 0.001$, $\eta^2_p = 0.69$), AREA*BAND ($F_{(6348)} = 93.31$, $p_{GG} < 0.001$, $\eta^2_p = 0.62$), AREA*HEMISPHERE ($F(3174) = 3.78$, $p_{GG} = 0.020$, $\eta^2_p=0.06$), BAND*HEMISPHERE ($F_{(2116)}=8.99$, $p_{GG}<0.001$, $\eta^2_p=0.13$), CONDITION*HEMISPHERE ($F_{(1,58)} = 6.30$, $p = 0.015$, $\eta^2_p = 0.10$), AREA*BAND*CONDITION ($F_{(6348)} = 28.68$, $p_{GG} < 0.001$, $\eta^2_p = 0.33$).

Age-related effects. The AGE*AREA interaction was further evaluated by comparing age differences within the same area (see Supplementary Materials – Table S1 for statistical details, and Fig. 2). Power values in older adults were higher than in young individuals in frontal ($t_{(174)}=6.09$, $p_{adj}<0.001$, $d = 0.46$), parietal ($t_{(174)}=3.21$, $p_{adj}=0.002$, $d = 0.24$) and temporal ($t_{(174)}=7.54$, $p_{adj}<0.001$, $d = 0.57$) areas, while the opposite holds for the occipital area ($t_{(174)}=-16.85$, $p_{adj}<0.001$, $d = 1.28$). Namely, power distribution changed with age: while the occipital area exhibited higher power in young individuals, the parietal, temporal and frontal areas, on the contrary, showed higher power in older adults. Overall, these age-related changes in power agree with the predictions of the PASA model: in older adults, we observe a power shift from the occipital areas to the more anterior areas.

Age-unrelated effects. See supplementary materials.

3.2. Connectivity

3.2.1. Inter-area connectivity via CTO

To study age-related modulation of inter-area connectivity we analyzed each pair of areas separately, with area-related connectivity coefficients C_{AB} (see Section 2.3) as dependent variables and AGE as between-subjects factor for the ANOVA. In the case of inter-area connectivity between different areas belonging to the same hemisphere, the within-subjects factors were CONDITION, BAND and HEMISPHERE, while in the case of inter-area connectivity between homologous areas belonging to opposite hemispheres, within-subjects factors were CONDITION and BAND.

A significant effect of AGE was detected in the frontal-parietal ($F_{(1,58)}=7.82$, $p = 0.007$, $\eta^2_p=0.12$), frontal-temporal ($F_{(1,58)}=7.53$, $p = 0.008$, $\eta^2_p=0.12$) and parietal-temporal ($F_{(1,58)}=5.75$, $p = 0.020$, $\eta^2_p=0.09$) connectivity, as well as in the occipital left-right connectivity ($F_{(1,58)}=7.82$, $p = 0.007$, $\eta^2_p=0.12$). These effects are the most interesting for the present investigation and are further discussed in detail below. A significant CONDITION effect was found in occipital-parietal ($F_{(1,58)}=35.11$, $p<0.001$, $\eta^2_p=0.38$) and occipital-temporal ($F_{(1,58)}=21.08$, $p<0.001$, $\eta^2_p=0.27$) connectivity. All considered pairs of areas gave a significant main BAND effect (all Fs>11.3, all ps<0.001, see Supplementary Materials – Table S5). The ANOVA on frontal-temporal connectivity showed a significant BAND*AGE interaction ($F_{(2116)}=11.34$, $p<0.001$, $\eta^2_p=0.16$) and a significant BAND*CONDITION*AGE interaction ($F_{(2116)}=3.38$, $p = 0.037$, $\eta^2_p=0.06$). In seven cases out of ten, a significant BAND*CONDITION interaction emerged. Finally, significant BAND*HEMISPHERE ($F_{(2116)}=8.54$, $p_{GG}<0.001$, $\eta^2_p=0.13$) and CONDITION*HEMISPHERE ($F_{(1,58)}=4.66$, $p = 0.035$, $\eta^2_p=0.07$) interactions were found in the case of occipito-temporal connectivity.

Age-related effects. As reported above, the main effect of AGE indicated that connectivity in older adults was significantly higher than in young individuals in the case of frontal-parietal ($p = 0.007$), frontal-temporal ($p = 0.008$) and parietal-temporal ($p = 0.020$) connectivity (Fig. 3). In contrast, in the case of occipital left-right connectivity, young adults exhibited a higher connectivity with respect to older ones ($p = 0.007$; see Fig. 3).

From the analysis of frontal-temporal connectivity, significant BAND*AGE and AGE*BAND*CONDITION interactions were found. We followed-up this latter interaction, focusing on differences between age groups for each level of BAND and CONDITION. As a result, older adults exhibited higher connectivity in EC condition theta ($t_{(116)}=3.112$, $p_{adj}=0.005$, $d = 0.29$) and alpha band ($t_{(116)}=3.158$, $p_{adj}=0.005$, $d = 0.29$), and in EO condition theta ($t_{(116)}=3.989$, $p_{adj}<0.001$, $d = 0.37$) and alpha band ($t_{(116)}=3.379$, $p_{adj}=0.003$, $d = 0.31$). In other words, the pattern highlighted by the AGE effect for frontal-temporal connectivity appears to be driven by the alpha and theta bands.

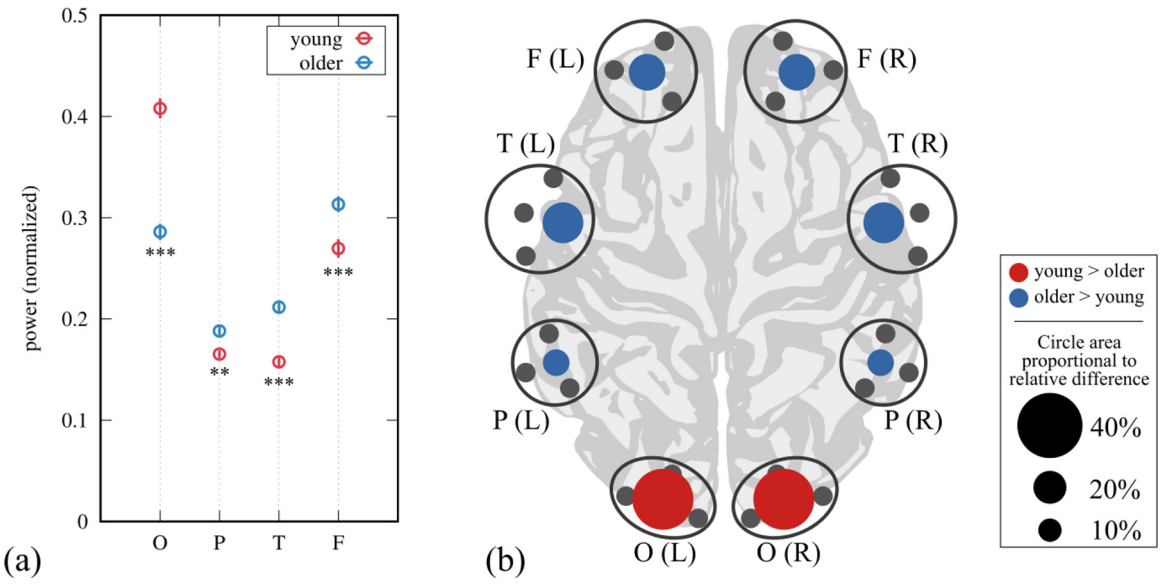

Fig. 2. Results of the analysis of power distribution among areas. (a) Multiple comparisons of age groups and of different areas. Dots and errorbars correspond to averages values and the related standard errors. Significant differences are marked by one ($p < 0.05$), two ($p < 0.01$) or three asterisks ($p < 0.001$). Area abbreviations: O = Occipital, P = Parietal, T = Temporal, F = Frontal; L = Left, R = Right. (b) Graphical summary of significant power differences between age groups on an approximate brain diagram reporting the 24 nodes (gray dots) considered here. Colored circles represent significant differences between age groups. Circle area is proportional to the relative difference in power between the groups; circle color corresponds to the group with largest power.

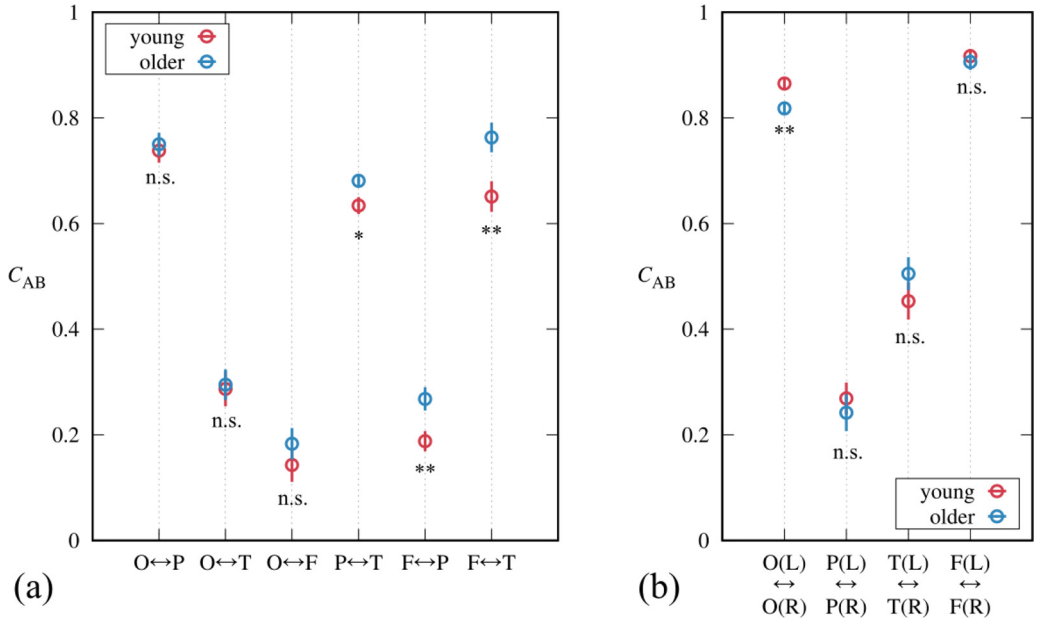

Fig. 3. Post-hoc comparisons of the results of inter-area connectivity estimates based on the CTO method as a function of age and area. Dots and error bars correspond to averages values and the related standard errors. Significant differences are marked by one ($p < 0.05$), two ($p < 0.01$) or three asterisks ($p < 0.001$). Area abbreviations: O = Occipital, P = Parietal, T = Temporal, F = Frontal; L = Left, R = Right. (a) Connectivity between different areas belonging to the same hemisphere. (b) Connectivity between homologous areas in opposite hemispheres.

To summarize, inter-area connectivity was stronger in older adults with respect to young individuals for every pair of areas not including the occipital area. However, inter-area connectivity was weaker in older adults with respect to young adults when the left-right occipital pair was considered.

Age-unrelated effects. See supplementary materials.

3.2.2. Intra-area connectivity via MI

To investigate intra-area connectivity, the results of MI were analyzed by considering the area-related mutual information values MI_{AA} (see Section 2.3) as dependent variables and by carrying out a mixed ANOVA (bs: AGE; ws: CONDITION, BAND, AREA, HEMISPHERE). The test yielded the following significant effects: AGE ($F_{(1,58)}$=4.92, p = 0.030, η^2_p=0.08), BAND ($F_{(2116)}$=41.05, p<0.001, η^2_p=0.41), CONDITION ($F_{(1,58)}$=31.83, p<0.001, η^2_p=0.35), AREA ($F_{(3174)}$=320.89, p_{GG}<0.001, η^2_p=0.85), HEMISPHERE ($F_{(1,58)}$=4.13, p<0.001, η^2_p=0.69), AGE*AREA ($F_{(3174)}$=16.78, p_{GG}<0.001, η^2_p=0.22), AREA*HEMISPHERE ($F_{(3174)}$=152.23, p_{GG}<0.001, η^2_p=0.72), BAND*CONDITION ($F_{(2116)}$=19.34, p_{GG}<0.001, η^2_p=0.25), AREA*CONDITION ($F_{(3174)}$=38.11, p_{GG}<0.001, η^2_p=0.40), and AREA*BAND*CONDITION ($F_{(6348)}$=9.08, p_{GG}<0.001, η^2_p=0.14).

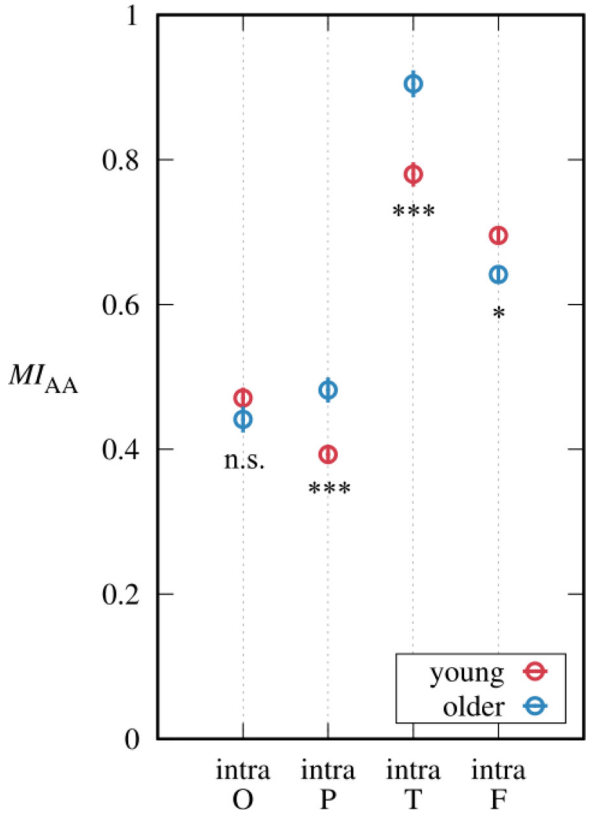

Fig. 4. Post-hoc comparisons of the results of intra-area connectivity estimates based on MI as a function of age and involved area. Dots and error bars correspond to averages values and the related standard errors. Significant differences are marked by one ($p < 0.05$), two ($p < 0.01$) or three asterisks ($p < 0.001$). Area abbreviations: O = Occipital, P = Parietal, T = Temporal, F = Frontal.

Age-related effects. The main effect of AGE shows that older adults exhibit, overall, a significantly stronger intra-area connectivity with respect to young adults. Follow-up analyses (t-tests) for the significant AGE*AREA interaction indicated that older individuals exhibited a significantly stronger intra-area connectivity in the parietal ($t_{(174)}$=3.77, p_{adj}<0.001, d = 0.29) and temporal ($t_{(174)}$=5.28, p_{adj}<0.001, d = 0.40) areas (Fig. 4). Conversely, the intra-area connectivity of older individuals in the frontal area was significantly weaker than the one observed for young individuals ($t_{(174)}$=−2.28, p_{adj}=0.028, d = 0.17, Fig. 4). To summarize, opposite patterns were observed in young and old individuals, with the frontal area more strongly connected in young adults, and temporal/parietal areas more strongly connected in older adults.

Age-unrelated effects. See supplementary materials.

3.2.3. Combined CTO/MI results

In the following, the results provided by the CTO method and MI are combined to give a complete overview of connectivity changes with age. A graphical summary of the differences in connectivity between age groups, obtained by combining together the results stemming from the CTO and MI methods presented above, is shown in Fig. 5: inter-area connectivity is evaluated through CTO data (Fig. 3(a-b)), while intra-area connectivity is evaluated via MI data (Fig. 4). The graph shows significant differences by means of lines either connecting different areas (inter-area) or connecting nodes within an area (intra-area). The corresponding line thickness is proportional to the relative difference in connectivity between groups, namely the difference between the averaged C_{AB} or MI_{AA} coefficients of the two age groups divided by the average of the two values. Line color identifies the group exhibiting the strongest connectivity. The results summarized in Fig. 5 complement the information provided by the analysis of power of Fig. 2. Specifically, on the one hand the larger power within the parietal and temporal areas detected for older adults (Fig. 2, blue circles) appears to be related to stronger intra-area connectivity within those two areas (Fig. 5, blue lines). On the other hand, the larger power within the frontal areas (Fig. 2, blue circles) is not: here the intra-area connectivity is stronger for young individuals (Fig. 5, red lines). Therefore, while the larger parietal and temporal power in older adults is due to an increase in both intra-area and inter-area connectivity, the larger frontal power is mainly due to an increased inter-area connectivity between the frontal area and the parietal/temporal areas of older adults.

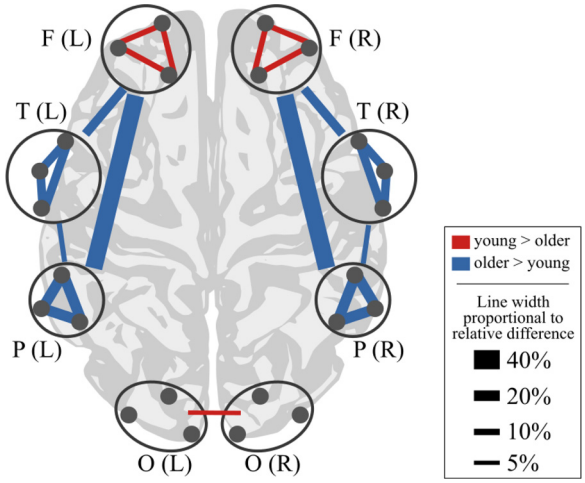

Fig. 5. Graphical summary of the significant differences in connectivity between young and older adults on an approximate brain diagram reporting the 24 nodes (gray dots) considered here. Area abbreviations: O = Occipital, P = Parietal, T = Temporal, F = Frontal; L = Left, R = Right. Lines between areas or within nodes of a given area represent significant differences in connectivity. Line colors identify which group exhibits the largest connectivity and line thickness is proportional to the relative difference in connectivity between groups. Connectivity is evaluated as the C_{AB} coefficient for inter-area connectivity (lines between areas), and as MI_{AA} for intra-area connectivity (lines within areas).

3.3. Modularity

Modularity was computed for ten values of the c_t threshold (see Section 2.4) from 0 to 0.9 in steps of 0.1, to check for possible effects due to the arbitrary choice of the threshold. For each threshold value, an ANOVA (bs: AGE; ws: CONDITION, BAND) was carried out by considering the modularity Q as dependent variable. A significant AGE main effect was found for all threshold values. In addition, significant BAND and CONDITION main effects were also found, as well as a significant BAND*CONDITION interaction detected for all $c_t \geq 0.3$. Finally, only for $c_t = 0.9$, a significant AGE*BAND*CONDITION interaction was found. Statistical details concerning these findings are reported in the Supplementary Materials (Tables S12, S13).

Main AGE effect. As far as the main AGE effect is concerned, for any value of the threshold, young adults exhibited significantly higher modularity than older individuals (Fig. 6) highlighting that the difference between age groups is independent of the threshold c_t. The significant AGE*BAND*CONDITION interaction detected only in the case of $c_t = 0.9$ ($F_{(2116)}$=4.43, p = 0.014, η^2_p=0.07) shows that young individuals exhibit a higher modularity than older adults only for theta-EC ($t_{(116)}$=−2.64, p_{adj}=0.017, d = 0.25), theta-EO ($t_{(116)}$=−2.94, p_{adj}=0.008, d = 0.27) and alpha-EO ($t_{(116)}$=−2.99, p_{adj}=0.007, d = 0.28). This result, however, might also be spurious due to a too high threshold ($c_t = 0.9$) leading to the selection of very few links.

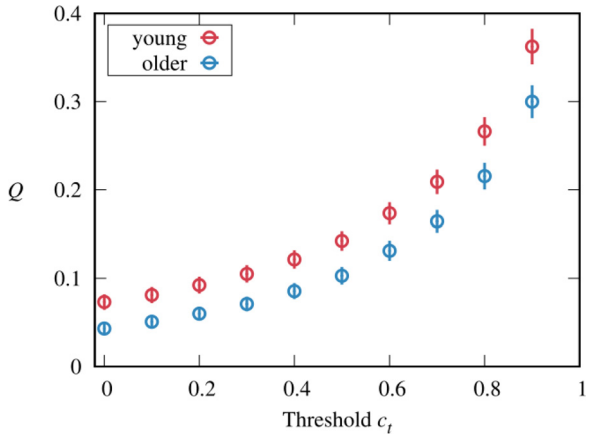

Fig. 6. Age-group averaged modularity (Q) as a function of threshold c_t. Dots and error bars correspond to averages values and the related standard errors.

Age-unrelated effects. See supplementary materials.

4. Discussion

In the present study, we investigated whether the patterns of EEG activity extracted from resting state support age-related changes predicted by PASA and HAROLD accounts. To evaluate the contribution of intra- and inter-area neural changes related to aging, we focused on connectivity measures, in addition to the more traditional measures of power.

We found that young individuals exhibited higher power (across all frequency ranges) in the occipital area as opposed to the relatively higher power showed by older adults in the parietal, temporal and frontal areas. This result is consistent with the activations described by the PASA model (Davis et al., 2008), which predicts a shift of brain activation with age from posterior to (more) anterior areas. Although the model was formulated by relying on task-based fMRI measures, we observed here an analogous pattern of changes in resting-state and by using EEG data. The present results are (partially) in line with other resting-state M/EEG studies in aging. For instance, previous studies have also shown increased theta power over occipital areas in younger adults, while theta oscillatory activity was less spatially differentiated over anterior and posterior sites (Puligheddu et al., 2005) or overall reduced in posterior electrodes (Barry and De Blasio, 2017) for older individuals. Reduction of alpha band activity in older adults was instead evident in occipital areas (Barry and De Blasio, 2017; Babiloni et al., 2006) and increased beta was found over frontal areas of older adults (Barry and De Blasio, 2017).

Crucially, we integrated the information derived from the power distribution across the brain by investigating connectivity with CTO and MI, two complementary methods that capitalize on the fine temporal resolution of EEG recordings. The results provide new insight on the mechanisms underlying the observed power shift. Specifically, the main finding of CTO was an increase, for older individuals, in inter-area connectivity involving the parietal, temporal and frontal areas. This result could account for the observed age-related power shift in terms of a more integrated connectivity across the three areas. In addition to CTO results, MI indicated an increased intra-area connectivity in the parietal and temporal areas in older adults, in line with the age-related increase in power observed in temporal/parietal areas. In the frontal area, on the other hand, the opposite effect was observed: while power increased with age, a decrease of intra-area connectivity was detected. This observation leads to the conclusion that, while the increase in power exhibited in older adults within temporal and parietal areas is associated both to intra-area and inter-area connectivity, in the case of the frontal area the increase in power seems mostly due to inter-area—rather than intra-area—connectivity between the frontal area and the temporal/parietal ones. These results resonate, for example, with the age-related decrease in frontal homotopic connectivity and the age-related increase in fronto-parietal connectivity observed by previous studies (Zangrossi et al., 2021) through the analysis of sensor-space EEG recordings. The increased fronto-temporal connectivity that we observed was also found in an fMRI study during a memory encoding task (Oh and Jagust, 2013). Another fMRI study, during a working memory task, reported an increased engagement between frontal and parietal areas (Mätthaus et al., 2012). Despite the present sample of older adults included only cognitively fit individuals, the overall increase in connectivity observed here might also be referred to the framework of hyperconnectivity (Hillary and Grafman, 2017), namely an enhanced connectivity between brain regions that was observed in early stages of mild cognitive impairment while waning in later stages, and that was suggested to be a mechanism of plasticity (Bonanni et al., 2021).

Finally, we analyzed how the observed age-related changes in connectivity affect the global topology of the network, quantified in terms of modularity. Regardless of the threshold used to build the network adjacency matrix, we systematically observed a lower modularity in older adults. This result suggests that older individuals exhibit less segregated network structures, since the different modules (i.e. areas) are more strongly interconnected. A decreased modularity with age was detected also in previous works, both relying on resting-state fMRI (Geerligs et al., 2015; Song et al., 2014) and EEG (Knyazev et al., 2015), and is consistent with a general shift towards a more random topology—and a decreasing segregation—of brain networks with age (Gaál et al., 2010; Zangrossi et al., 2021). In previous works, higher levels of modularity (i.e., greater network organization) have been related to better cognitive performance, for example correlating with higher gain after cognitive training (Arnemann et al., 2015; Baniqued et al., 2018). In the context of aging, and in line with a de-differentiation view of the aging process (Koen and Rugg, 2019), some works reported a lower degree of segregation in older adults (Song et al., 2014; Geerligs et al., 2015), thus suggesting that the overall worse cognitive performance of older adults might be due to a less segregated (i.e., less organized) network structure. While no direct link between modularity and performance can be investigated in the context of resting-state data, our results contribute to the growing body of evidence concerning reduced modularity in healthy aging.

Overall, the present findings of an age-related posterior-anterior effect are in line with the PASA model (Davis et al., 2008). Hemisphere-related modulations were essentially absent, thus ruling out asymmetry-reduction patterns as predicted by the HAROLD model (Cabeza, 2002). Indeed, a previous attempt to match the HAROLD model with resting-state fMRI observations was also inconclusive (Li et al., 2009). Nevertheless, it should be pointed out that the present investigation was based on resting-state recordings: it might be the case that asymmetry-related effects in aging are mostly evident during task execution (Mazza and Pagano, 2017), while they are too small to be detected in a resting-state condition. For instance, it was shown that the direction and degree of lateralization depends on task load during an attention task (Pérez et al., 2009), in line with the idea that attentional processes are lateralized (Rushworth et al., 2001). On the other hand, resting-state networks are typically found to be symmetric between hemispheres (Smith et al., 2009; Tyszka et al., 2011), although asymmetries were detected, for instance, in language areas (Raemaekers et al., 2018) and a few other areas (Di et al., 2014).

We analyzed source-space activity in three frequency bands that are typically considered in aging studies, namely theta, alpha, and beta (Puligheddu et al., 2005; Stacey et al., 2021; Chow et al., 2022). Because the goal of the present work was to investigate the effects of healthy aging on resting-state EEG activity, we focused our discussion on the statistical effects and interactions that involved the age factor. The band factor was found to significantly interact with age only in the case of frontal-temporal connectivity (significant AGE*BAND*CONDITION in-

teraction), for which the follow-up analysis revealed that connectivity differences between young and older adults are mostly contributed by the theta and alpha bands. Similar remarks can be drawn for the role of condition: no relevant interaction between age and condition was found, in line with previous EEG studies (Barry and De Blasio, 2017; Stacey et al., 2021). Overall, the lack of a systematic significant interaction between age, band and condition suggests that the effects observed in the present study were not frequency-specific.

Our investigation did not concern task-related EEG recordings, where functional connections are modulated by the specific task at hand (Di et al., 2014). Previous studies showed that resting-state connectivity between two regions correlates with the co-activation strength of the two regions during tasks (Toro et al., 2008; Di et al., 2014). Consequently, the analysis of rest data—as it was done in the present work—allows to assess brain connectivity in a more general way, probing several functional dynamics states (Smith et al., 2009). Thus, the use of resting-state recording can provide, with respect to task-based recordings, a complementary perspective on the effects of aging on default brain activity, highlighting the existence of more general phenomena. In contrast, the absence of a task does not allow to study the relationship between the observed electrophysiological variables and task performance. Consequently, it is not possible to relate the changes in power and connectivity observed here either to a compensatory or to a de-differentiation mechanism. This limitation also implies that more complex models of neurocognitive aging, such as the compensation-related utilization of neural circuits hypothesis (CRUNCH) (Reuter-Lorenz and Cappell, 2008), which predicts over-activation in older adults at lower levels of task difficulty, cannot be tested in the context of resting-state data. To this purpose, future studies should be directed towards acquiring, for the same participants, both resting-state and task-based recordings, possibly probing different domains of cognition.

To conclude, in partial agreement with our hypothesis, we showed that resting-state EEG presents patterns of age-related changes of brain activity supporting the PASA model, thus providing further evidence and extending the domain of validity of the model. On the contrary, we found no support of the HAROLD model in resting-state EEG. Furthermore, we found age-related changes in connectivity associated with the observed shift of power. Overall, these changes can be summarized as a loss of segregation of the network (i.e., a decrease in modularity), as parietal, temporal and frontal areas become more interconnected with each other, while frontal intra-area connectivity is diminished. These outcomes provide additional insights into the investigation of the mechanisms that drive age-related changes in brain activity.

Data and code availability

EEG recordings used in the present work are publicly available in the LEMON database at http://fcon_1000.projects.nitrc.org/indi/retro/MPI_LEMON.html (see also Babayan et al. (2019)).

Code for the CTO method is available in the open-source NetOnZeroDXC package (see Perinelli and Ricci, 2019). Auxiliary code is available from the corresponding author upon request.

Declaration of Competing Interest

The authors declare the following financial interests/personal relationships which may be considered as potential competing interests:

A patent application titled “Improving cognitive functions” has been submitted by the University of Birmingham and Dalhousie University with SA figuring as one of the inventors.

Credit authorship contribution statement

Alessio Perinelli: Conceptualization, Methodology, Software, Formal analysis, Writing – original draft. **Sara Assecondi:** Methodology, Supervision, Writing – review & editing. **Chiara F. Tagliabue:** Supervision, Writing – review & editing. **Veronica Mazza:** Conceptualization, Methodology, Supervision, Writing – review & editing.

Acknowledgments

AP and SA are supported by the Fondazione Cassa Di Risparmio Di Trento e Rovereto (CARITRO).

Supplementary materials

Supplementary material associated with this article can be found, in the online version, at doi:10.1016/j.neuroimage.2022.119247.

References

Andrews-Hanna, J.R., Snyder, A.Z., Vincent, J.L., Lustig, C., Head, D., Raichle, M.E., Buckner, R.L., 2007. Disruption of Large-Scale Brain Systems in Advanced Aging. Neuron 56, 924–935. doi:10.1016/j.neuron.2007.10.038.

Ansado, J., Monchi, O., Ennabil, N., Faure, S., Joanette, Y., 2012. Load-dependent posterior-anterior shift in aging in complex visual selective attention situations. Brain Res 1454, 14–22. doi:10.1016/j.brainres.2012.02.061.

Arnemann, K.L., Chen, A.J.-W., Novakovic-Agopian, T., Gratton, C., Nomura, E.M., D'Esposito, M., 2015. Functional brain network modularity predicts response to cognitive training after brain injury. Neurology 84, 1568–1574. doi:10.1212/WNL.0000000000001476.

Babayan, A., Erbey, M., Kumral, D., Reinelt, J.D., Reiter, A.M.F., Röbbig, J., Schaare, H.L., Uhlig, M., Anwander, A., Bazin, P.-.L., Horstmann, A., Lampe, L., Nikulin, V.V., Okon-Singer, H., Preusser, S., Pampel, A., Rohr, C.S., Sacher, J., Thöne-Otto, A., Trapp, S., Nierhaus, T., Altmann, D., Arelin, K., Blöchl, M., Bongartz, E., Breig, P., Cesnaite, E., Chen, S., Cozatl, R., Czerwonatis, S., Dambrauskaite, G., Dreyer, M., Enders, J., Engelhardt, M., Fischer, M.M., Forschack, N., Golchert, J., Golz, L., Guran, C.A., Hedrich, S., Hentschel, N., Hoffmann, D.I., Huntenburg, J.M., Jost, R., Kosatschek, A., Kunzendorf, S., Lammers, H., Lauckner, M.E., Mahjoory, K., Kanaan, A.S., Mendes, N., Menger, R., Morino, E., Näthe, K., Neubauer, J., Noyan, H., Oligschläger, S., Panczyszyn-Trzewik, P., Poehlchen, D., Putzke, N., Roski, S., Schaller, M.-.C., Schieferbein, A., Schlaak, B., Schmidt, R., Gorgolewski, K.J., Schmidt, H.M., Schrimpf, A., Stasch, S., Voss, M., Wiedemann, A., Margulies, D.S., Gaebler, M., Villringer, A., 2019. A mind-brain-body dataset of MRI, EEG, cognition, emotion, and peripheral physiology in young and old adults. Sci. Data 6. doi:10.1038/sdata.2018.308.

Babiloni, C., Binetti, G., Cassarino, A., Dal Forno, G., Del Percio, C., Ferreri, F., Ferri, R., Frisoni, G., Galderisi, S., Hirata, K., Lanuzza, B., Miniussi, C., Mucci, A., Nobili, F., Rodriguez, G., Luca Romani, G., Rossini, P.M., 2006. Sources of cortical rhythms in adults during physiological aging: a multicentric EEG study. Hum. Brain Mapp. 27, 162–172. doi:10.1002/hbm.20175.

Balsters, J.H., O'Connell, R.G., Galli, A., Nolan, H., Greco, E., Kilcullen, S.M., Bokde, A.L.W., Lai, R., Upton, N., Robertson, I.H., 2013. Changes in resting connectivity with age: a simultaneous electroencephalogram and functional magnetic resonance imaging investigation. Neurobiol. Aging 34, 2194–2207. doi:10.1016/j.neurobiolaging.2013.03.004.

Baniqued, P.L., Gallen, C.L., Voss, M.W., Burzynska, A.Z., Wong, C.N., Cooke, G.E., Duffy, K., Fanning, J., Ehlers, D.K., Salerno, E.A., Aguiñaga, S., McAuley, E., Kramer, A.F., D'Esposito, M., 2018. Brain network modularity predicts exercise-related executive function gains in older adults. Front. Aging Neurosci. 9, 426. doi:10.3389/fnagi.2017.00426.

Barry, R.J., De Blasio, F.M., 2017. EEG differences between eyes-closed and eyes-open resting remain in healthy ageing. Biol. Psychol. 129, 293–304. doi:10.1016/j.biopsycho.2017.09.010.

Bastos, A.M., Schoffelen, J.M., 2016. A tutorial review of functional connectivity analysis methods and their interpretational pitfalls. Fron. Sys. Neurosci 9, 175. doi:10.3389/fnsys.2015.00175.

Benjamini, Y., Yekutieli, D., 2001. The control of the false discovery rate in multiple testing under dependency. Ann. Statist. 29. doi:10.1214/aos/1013699998.

Blanca, M.J., Alarcón, R., Arnau, J., Bono, R., Bendayan, R., 2018. Effect of variance ratio on ANOVA robustness: might 1.5 be the limit? Behav Res 50, 937–962. doi:10.3758/s13428-017-0918-2.

Bonanni, L., Moretti, D., Benussi, A., Ferri, L., Russo, M., Carrarini, C., Barbone, F., Arnaldi, D., Falasca, N.W., Koch, G., Cagnin, A., Nobili, F., Babiloni, C., Borroni, B., Padovani, A., Onofrj, M., Franciotti, R.the FTD Italian study group-SINDEM, 2021. Hyperconnectivity in dementia is early and focal and wanes with progression. Cerebral Cortex 31, 97–105. doi:10.1093/cercor/bhaa209.

Bowyer, S.M., 2016. Coherence a measure of the brain networks: past and present. Neuropsychiatric Electrophysiology 2, 1. doi:10.1186/s40810-015-0015-7.

Brunner, C., Billinger, M., Seeber, M., Mullen, T.R., Makeig, S., 2016. Volume conduction influences scalp-based connectivity estimates. Front Comput. Neurosci. 10. doi:10.3389/fncom.2016.00121, 121–121.

Cabeza, R., 2002. Hemispheric asymmetry reduction in older adults: the HAROLD model. Psychol. Aging 17. doi:10.1037/0882-7974.17.1.85.

Cabeza, R., Dennis, N.A., 2012. Frontal lobes and aging: deterioration and compensation. In: Stuss, D.T., Knight, R.T. (Eds.), Principles of Frontal Lobe Function. Oxford University Press, New York, pp. 628–652.

Cabeza, R., Grady, C.L., Nyberg, L., McIntosh, A.R., Tulving, E., Kapur, S., Jennings, J.M., Houle, S., Craik, F.I.M., 1997. Age-related differences in neural activity during memory encoding and retrieval: a positron emission tomography study. J. Neurosci. 17. doi:10.1523/JNEUROSCI.17-01-00391.1997, 391 LP –400.

Cabral, J., Vidaurre, D., Marques, P., Magalhães, R., Silva Moreira, P., Miguel Soares, J., Deco, G., Sousa, N., Kringelbach, M.L., 2017. Cognitive performance in healthy older adults relates to spontaneous switching between states of functional connectivity during rest. Sci. Rep. 7. doi:10.1038/s41598-017-05425-7, 5135–5135.

Castelluzzo, M., Perinelli, A., Tabarelli, D., Ricci, L., 2021. Dependence of connectivity on the logarithm of geometric distance in brain networks. Front Physiol. 11. doi:10.3389/fphys.2020.611125.

Chang, C., Liu, Z., Chen, M.C., Liu, X., Duyn, J.H., 2013. EEG correlates of time-varying BOLD functional connectivity. Neuroimage 72, 227–236. doi:10.1016/j.neuroimage.2013.01.049.

Chan, M.Y., Park, D.C., Savalia, N.K., Petersen, S.E., Wig, G.S., 2014. Decreased segregation of brain systems across the healthy adult lifespan. Proc. Natl. Acad. Sci. USA 111, E4997–E5006. doi:10.1073/pnas.1415122111.

Chiang, A.K.I., Rennie, C.J., Robinson, P.A., van Albada, S.J., Kerr, C.C., 2011. Age trends and sex differences of alpha rhythms including split alpha peaks. Clin. Neurophysiol. 122, 1505–1517. doi:10.1016/j.clinph.2011.01.040.

Chow, R., Rabi, R., Paracha, S., Hasher, L., Anderson, N.D., Alain, C., 2022. Default mode network and neural phase synchronization in healthy aging: a resting state EEG study. Neuroscience 485, 116–128. doi:10.1016/j.neuroscience.2022.01.008.

Cover, T.M., Thomas, J.A., 2006. Elements of Information Theory, 2nd ed. Wiley-Interscience, Hoboken, N.J ed..

Crouch, B., Sommerlade, L., Veselicic, P., Riedel, G., Schelter, B., Platt, B., 2018. Detection of time-, frequency- and direction-resolved communication within brain networks. Sci. Rep. 8, 1825. doi:10.1038/s41598-018-19707-1.

Cummins, T.D.R., Finnigan, S., 2007. Theta power is reduced in healthy cognitive aging. Int. J. Psychophysiol. 66, 10–17. doi:10.1016/j.ijpsycho.2007.05.008.

Damoiseaux, J.S., Beckmann, C.F., Arigita, E.J.S., Barkhof, F., Scheltens, Ph., Stam, C.J., Smith, S.M., Rombouts, S.A.R.B., 2008. Reduced resting-state brain activity in the "default network" in normal aging. Cerebral Cortex 18, 1856–1864. doi:10.1093/cercor/bhm207.

Davis, S.W., Dennis, N.A., Daselaar, S.M., Fleck, M.S., Cabeza, R., 2008. Que PASA? The posterior-anterior shift in aging. Cerebral Cortex 18. doi:10.1093/cercor/bhm155.

Dennis, N.A., Cabeza, R., 2008. Neuroimaging of healthy cognitive aging. In: Craik, F.I.M., Salthouse, T.A. (Eds.), The Handbook of Aging and Cognition. Psychology Press, pp. 1–54.

D'Esposito, M., Deouell, L.Y., Gazzaley, A., 2003. Alterations in the BOLD fMRI signal with ageing and disease: a challenge for neuroimaging. Nature Reviews Neuroscience 4, 863–872. doi:10.1038/nrn1246.

Di, X., Kim, E.H., Chen, P., Biswal, B.B., 2014. Lateralized resting-state functional connectivity in the task-positive and task-negative networks. Brain Connect 4, 641. doi:10.1089/brain.2013.0215.

Dolcos, F., Rice, H.J., Cabeza, R., 2002. Hemispheric asymmetry and aging: right hemisphere decline or asymmetry reduction. Neuroscience & Biobehavioral Reviews 26, 819–825. doi:10.1016/S0149-7634(02)00068-4.

Escrichs, A., Biarnes, C., Garre-Olmo, J., Fernández-Real, J.M., Ramos, R., Pamplona, R., Brugada, R., Serena, J., Ramió-Torrentà, L., Coll-De-Tuero, G., Gallart, L., Barretina, J., Vilanova, J.C., Mayneris-Perxachs, J., Essig, M., Figley, C.R., Pedraza, S., Puig, J., Deco, G., 2021. Whole-brain dynamics in aging: disruptions in functional connectivity and the role of the rich club. Cerebral Cortex 31, 2466–2481. doi:10.1093/cercor/bhaa367.

Eyler, L.T., Sherzai, A., Kaup, A.R., Jeste, D.V., 2011. A review of functional brain imaging correlates of successful cognitive aging. Biol. Psych. 70, 115–122. doi:10.1016/j.biopsych.2010.12.032.

Fabiani, M., 2012. It was the best of times, it was the worst of times: a psychophysiologist's view of cognitive aging. Psychophysiology 49, 283–304. doi:10.1111/j.1469-8986.2011.01331.x.

Festini, S.B., Zahodne, L., Reuter-Lorenz, P.A., 2018. Theoretical perspectives on age differences in brain activation: HAROLD, PASA, CRUNCH—how do they stac up? doi:10.1093/acrefore/9780190236557.013.400.

Finnigan, S., Robertson, I.H., 2011. Resting EEG theta power correlates with cognitive performance in healthy older adults: resting theta EEG correlates with cognitive aging. Psychophysiology 48, 1083–1087. doi:10.1111/j.1469-8986.2010.01173.x.

Fleck, J.I., Kuti, J., Mercurio, J., Mullen, S., Austin, K., Pereira, O., 2017. The impact of age and cognitive reserve on resting-state brain connectivity. Front Aging Neurosci. 9. doi:10.3389/fnagi.2017.00392, 392–392.

Gaál, Z.A., Boha, R., Stam, C.J., Molnár, M., 2010. Age-dependent features of EEG-reactivity—Spectral, complexity, and network characteristics. Neurosci. Lett. 479, 79–84. doi:10.1016/j.neulet.2010.05.037.

Gallen, C.L., D'Esposito, M., 2019. Brain modularity: a biomarker of intervention-related plasticity. Trends Cogn. Sci. (Regul. Ed.) 23. doi:10.1016/j.tics.2019.01.014.

Geerligs, L., Maurits, N.M., Renken, R.J., Lorist, M.M., 2014. Reduced specificity of functional connectivity in the aging brain during task performance: functional Connectivity in the Aging Brain. Hum. Brain Mapp 35, 319–330. doi:10.1002/hbm.22175.

Geerligs, L., Renken, R.J., Saliasi, E., Maurits, N.M., Lorist, M.M., 2015. A brain-wide study of age-related changes in functional connectivity. Cerebral Cortex 25, 1987–1999. doi:10.1093/cercor/bhu012.

Glass, G.V., Peckham, P.D., Sanders, J.R., 1972. Consequences of failure to meet assumptions underlying the fixed effects analyses of variance and covariance. Rev. Educ. Res. 42, 237–288. doi:10.3102/00346543042003237.

Glasser, M.F., Coalson, T.S., Robinson, E.C., Hacker, C.D., Harwell, J., Yacoub, E., Ugurbil, K., Andersson, J., Beckmann, C.F., Jenkinson, M., Smith, S.M., Van Essen, D.C., 2016. A multi-modal parcellation of human cerebral cortex. Nature 536, 171–178. doi:10.1038/nature18933.

Grady, C.L., 2012. The cognitive neuroscience of ageing. Nat. Rev. Neurosci. 13, 491–505. doi:10.1038/nrn3256.

Grady, C.L., Maisog, J.M., Horwitz, B., Ungerleider, L.G., Mentis, M.J., Salerno, J.A., Pietrini, P., Wagner, E., Haxby, J.V., 1994. Age-related changes in cortical blood flow activation during visual processing of faces and location. J. Neurosci. 14. doi:10.1523/JNEUROSCI.14-03-01450.1994, 1450 LP –1462.

Hedden, T., Gabrieli, J.D.E., 2004. Insights into the ageing mind: a view from cognitive neuroscience. Nat. Rev. Neurosci. 5, 87–96. doi:10.1038/nrn1323.

Heeger, D.J., Ress, D., 2002. What does fMRI tell us about neuronal activity? Nat. Rev. Neurosci 3, 142. doi:10.1038/nrn730.

Hillary, F.G., Biswal, B., 2007. The Influence of Neuropathology on the fMRI Signal: a Measurement of Brain or Vein? Clin. Neuropsychol. 21, 58–72. doi:10.1080/13854040601064542.

Hillary, F.G., Grafman, J.H., 2017. Injured brains and adaptive networks: the benefits and costs of hyperconnectivity. Trends Cogn. Sci. (Regul. Ed.) 21, 385–401. doi:10.1016/j.tics.2017.03.003.

Hrybouski, S., Cribben, I., McGonigle, J., Olsen, F., Carter, R., Seres, P., Madan, C.R., Malykhin, N.V., 2021. Investigating the effects of healthy cognitive aging on brain functional connectivity using 4.7 T resting-state functional magnetic resonance imaging. Brain Struc. Func. 226, 1067–1098. doi:10.1007/s00429-021-02226-7.

JASP team, 2021. JASP version 0.15, https://jasp-stats.org/ (accessed November 2021).

Jensen, O., Goel, P., Kopell, N., Pohja, M., Hari, R., Ermentrout, B., 2005. On the human sensorimotor-cortex beta rhythm: sources and modeling. Neuroimage 26, 347–355. doi:10.1016/j.neuroimage.2005.02.008.

Jeong, J., Gore, J.C., Peterson, B.S., 2001. Mutual information analysis of the EEG in patients with Alzheimer's disease. Clin. Neurophysiol. 112, 827–835. doi:10.1016/S1388-2457(01)00513-2.

Knyazev, G.G., Volf, N.V., Belousova, L.V., 2015. Age-related differences in electroencephalogram connectivity and network topology. Neurobiol. Aging 36, 1849–1859. doi:10.1016/j.neurobiolaging.2015.02.007.

Koen, J.D., Rugg, M.D., 2019. Neural Dedifferentiation in the Aging Brain. Trends Cogn. Sci. (Regul. Ed.) 23, 547–559. doi:10.1016/j.tics.2019.04.012.

Kozachenko, L.F., Leonenko, N.N., 1987. Sample estimate of the entropy of a random vector. Problems Inform. Transm. 23, 95–101.

Laufs, H., Krakow, K., Sterzer, P., Eger, E., Beyerle, A., Salek-Haddadi, A., Kleinschmidt, A., 2003. Electroencephalographic signatures of attentional and cognitive default modes in spontaneous brain activity fluctuations at rest. Proc. Natl. Acad. Sci. U.S.A. 100, 11053–11058. doi:10.1073/pnas.1831638100.

Learmonth, G., Benwell, C.S.Y., Thut, G., Harvey, M., 2017. Age-related reduction of hemispheric lateralisation for spatial attention: an EEG study. Neuroimage 153, 139–151. doi:10.1016/j.neuroimage.2017.03.050.

Leirer, V.M., Wienbruch, C., Kolassa, S., Schlee, W., Elbert, T., Kolassa, .I..-T., 2011. Changes in cortical slow wave activity in healthy aging. Brain Imaging Behav. 5, 222–228. doi:10.1007/s11682-011-9126-3.

Li, Z., Bacon Moore, A., Tyner, C., Hu, X., 2009. Asymmetric connectivity reduction and its relationship to "HAROLD" in aging brain. Brain Res 1295, 149. doi:10.1016/j.brainres.2009.08.004.

Li, H.J., Hou, X.H., Liu, H.H., Yue, C.L., Lu, G.M., Zuo, X.N., 2015. Putting age-related task activation into large-scale brain networks: a meta-analysis of 114 fMRI studies on healthy aging. Neurosci. Biobehav. Rev. 57, 156. doi:10.1016/j.neubiorev.2015.08.013.

Logothetis, N.K., Pauls, J., Augath, M., Trinath, T., Oeltermann, A., 2001. Neurophysiological investigation of the basis of the fMRI signal. Nature 412, 150. doi:10.1038/35084005.

Lombardi, D., Pant, S., 2016. Nonparametric *k*-nearest-neighbor entropy estimator. Phys. Rev. E 93. doi:10.1103/PhysRevE.93.013310, 13310–13310.

Matthäus, F., Schmidt, J.P., Banerjee, A., Schulze, T.G., Demirakca, T., Diener, C., 2012. Effects of age on the structure of functional connectivity networks during episodic and working memory demand. Brain Connect. 2, 113. doi:10.1089/brain.2012.0077.

Mazza, V., Pagano, S., 2017. Electroencephalographic asymmetries in human cognition. In: Rogers, L, Vallortigara, G (Eds.), Lateralized Brain Functions. Neuromethods. Humana Press, New York, NY vol 122.

McCarthy, P., Benuskova, L., Franz, E.A., 2014. The age-related posterior-anterior shift as revealed by voxelwise analysis of functional brain networks. Front Aging Neurosci. 6, 301. doi:10.3389/fnagi.2014.00301.

McIntosh, A.R., Vakorin, V., Kovacevic, N., Wang, H., Diaconescu, A., Protzner, A.B., 2014. Spatiotemporal dependency of age-related changes in brain signal variability. Cerebral Cortex 24, 1806–1817. doi:10.1093/cercor/bht030.

Michel, C.M., Brunet, D., 2019. EEG Source imaging: a practical review of the analysis steps. Front. Neurol. 10, 325. doi:10.3389/fneur.2019.00325.

Moezzi, B., Pratti, L.M., Hordacre, B., Graetz, L., Berryman, C., Lavrencic, L.M., Ridding, M.C., Keage, H.A.D., McDonnell, M.D., Goldsworthy, M.R., 2019. Characterization of young and old adult brains: an EEG functional connectivity analysis. Neuroscience 422, 230–239. doi:10.1016/j.neuroscience.2019.08.038.

Moosmann, M., Ritter, P., Krastel, I., Brink, A., Thees, S., Blankenburg, F., Taskin, B., Obrig, H., Villringer, A., 2003. Correlates of alpha rhythm in functional magnetic resonance imaging and near infrared spectroscopy. Neuroimage 20, 145–158. doi:10.1016/S1053-8119(03)00344-6.

Morcom, A.M., Johnson, W., 2015. Neural reorganization and compensation in aging. J. Cogn. Neurosci. 27, 1275–1285. doi:10.1162/jocn_a_00783.

Muthukumaraswamy, S.D., 2013. High-frequency brain activity and muscle artifacts in MEG/EEG: a review and recommendations. Front. Hum. Neurosci. 7. doi:10.3389/fnhum.2013.00138.

Newman, M.E.J., 2006. Modularity and community structure in networks. In: Proceedings of the National Academy of Sciences, 103 doi:10.1073/pnas.0601602103.
Newman, M.E.J., Girvan, M., 2004. Finding and evaluating community structure in networks. Phys. Rev. E 69. doi:10.1103/PhysRevE.69.026113, 26113–26113.
Oh, H., Jagust, W.J., 2013. Frontotemporal network connectivity during memory encoding is increased with aging and disrupted by beta-amyloid. J. Neurosci. 33, 18425. doi:10.1523/jneurosci.2775-13.2013.
Oostenveld, R., Fries, P., Maris, E., Schoffelen, .J..-M., 2011. FieldTrip: open source software for advanced analysis of MEG, EEG, and invasive electrophysiological data. Comput. Intell. Neurosci. 2011. doi:10.1155/2011/156869.
Oostenveld, R., Praamstra, P., 2001. The five percent electrode system for high-resolution EEG and ERP measurements. Clin. Neurophysiol. 112, 713–719. doi:10.1016/S1388-2457(00)00527-7.
Pascual-Marqui, R.D., Lehmann, D., Koukkou, M., Kochi, K., Anderer, P., Saletu, B., Tanaka, H., Hirata, K., John, E.R., Prichep, L., Biscay-Lirio, R., Kinoshita, T., 2011. Assessing interactions in the brain with exact low-resolution electromagnetic tomography. Philosoph. Transac. Royal Soc. A 369. doi:10.1098/rsta.2011.0081.
Pearson, E.S., 1931. The analysis of variance in cases of non-normal variation. Biometrika 23, 114. doi:10.1093/biomet/23.1-2.114.
Pérez, A., Peers, P.V., Valdés-Sosa, M., Galán, L., García, L., Martínez-Montes, E., 2009. Hemispheric modulations of alpha-band power reflect the rightward shift in attention induced by enhanced attentional load. Neuropsychologia 47, 41. doi:10.1016/j.neuropsychologia.2008.08.017.
Perinelli, A., Castelluzzo, M., Tabarelli, D., Mazza, V., Ricci, L., 2021. Relationship between mutual information and cross-correlation time scale of observability as measures of connectivity strength. Chaos 31. doi:10.1063/5.0053857.
Perinelli, A., Chiari, D.E., Ricci, L., 2018. Correlation in brain networks at different time scale resolution. Chaos 28. doi:10.1063/1.5025242.
Perinelli, A., Ricci, L., 2019. NetOnZeroDXC: a package for the identification of networks out of multivariate time series via zero-delay cross-correlation. SoftwareX 10. doi:10.1016/j.softx.2019.100316.
Perinelli, A., Tabarelli, D., Miniussi, C., Ricci, L., 2019. Dependence of connectivity on geometric distance in brain networks. Sci Rep 9. doi:10.1038/s41598-019-50106-2.
Pope, K.J., Fitzgibbon, S.P., Lewis, T.W., Whitham, E.M., Willoughby, J.O., 2009. Relation of gamma oscillations in scalp recordings to muscular activity. Brain Topogr. 22, 13–17. doi:10.1007/s10548-009-0081-x.
Pulighеddu, M., de Munck, J.C., Stam, C.J., Verbunt, J., de Jongh, A., van Dijk, B.W., Marrosu, F., 2005. Age distribution of MEG spontaneous theta activity in healthy subjects. Brain Topogr. 17, 165–175. doi:10.1007/s10548-005-4449-2.
Quian Quiroga, R., Panzeri, S., 2009. Extracting information from neuronal populations: information theory and decoding approaches. Nat. Rev. Neurosci. 10, 173–185. doi:10.1038/nrn2578.
Raemaekers, M., Schellekens, W., Petridou, N., Ramsey, N.F., 2018. Knowing left from right: asymmetric functional connectivity during resting state. Brain Struct. Funct. 223, 1909. doi:10.1007/s00429-017-1604-y.
Ren, P., Anthony, M., Aarsland, D., Wu, D., 2019. Commentary: a posterior-to-anterior shift of brain functional dynamics in aging. Front Aging Neurosci. 11, 341. doi:10.3389/fnagi.2019.00341.
Reuter-Lorenz, P.A., Cappell, K.A., 2008. Neurocognitive Aging and the Compensation Hypothesis. Curr. Dir. Psychol. Sci. 17, 177–182. doi:10.1111/j.1467-8721.2008.00570.x.
Reuter-Lorenz, P.A., Jonides, J., Smith, E.E., Hartley, A., Miller, A., Marshuetz, C., Koeppe, R.A., 2000. Age Differences in the Frontal Lateralization of Verbal and Spatial Working Memory Revealed by PET. J. Cogn. Neurosci. 12, 174–187. doi:10.1162/089892900561814.
Rieck, J.R., Baracchini, G., Nichol, D., Abdi, H., Grady, C.L., 2021. Reconfiguration and dedifferentiation of functional networks during cognitive control across the adult lifespan. Neurobiol. Aging 106, 80–94. doi:10.1016/j.neurobiolaging.2021.03.019.
Rossini, P.M., Di Iorio, R., Bentivoglio, M., Bertini, G., Ferreri, F., Gerloff, C., Ilmoniemi, R.J., Miraglia, F., Nitsche, M.A., Pestilli, F., Rosanova, M., Shirota, Y., Tesoriero, C., Ugawa, Y., Vecchio, F., Ziemann, U., Hallett, M., 2019. Methods for analysis of brain connectivity: an IFCN-sponsored review. Clin. Neurophysiol. 130, 1833–1858. doi:10.1016/j.clinph.2019.06.006.
Rushworth, M., Ellison, A., Walsh, V., 2001. Complementary localization and lateralization of orienting and motor attention. Nat. Neurosci. 4, 656. doi:10.1038/88492.
Sala-Llonch, R., Bartrés-Faz, D., Junqué, C., 2015. Reorganization of brain networks in aging: a review of functional connectivity studies. Front Psychol 6. doi:10.3389/fpsyg.2015.00663, 663–663.
Scally, B., Burke, M.R., Bunce, D., Delvenne, .J..-F., 2018. Resting-state EEG power and connectivity are associated with alpha peak frequency slowing in healthy aging. Neurobiol. Aging 71, 149–155. doi:10.1016/j.neurobiolaging.2018.07.004.
Scheeringa, R., Bastiaansen, M.C.M., Petersson, K.M., Oostenveld, R., Norris, D.G., Hagoort, P., 2008. Frontal theta EEG activity correlates negatively with the default mode network in resting state. Int. J. Psychophysiol. 67, 242–251. doi:10.1016/j.ijpsycho.2007.05.017.
Schneider-Garces, N.J., Gordon, B.A., Brumback-Peltz, C.R., Shin, E., Lee, Y., Sutton, B.P., Maclin, E.L., Gratton, G., Fabiani, M., 2010. Span, CRUNCH, and beyond: working memory capacity and the aging brain. J. Cognitive Neurosci 22, 655. doi:10.1162/jocn.2009.21230.
Schreiber, T., Schmitz, A., 2000. Surrogate time series. Physica D 142, 346–382. doi:10.1016/S0167-2789(00)00043-9.
Schreiber, T., Schmitz, A., 1996. Improved surrogate data for nonlinearity tests. Phys. Rev. Lett. 77, 635–638. doi:10.1103/PhysRevLett.77.635.
Shumbayawonda, E., Fernández, A., Hughes, M., Abásolo, D., 2017. Permutation entropy for the characterisation of brain activity recorded with magnetoencephalograms in healthy ageing. Entropy 19, 141. doi:10.3390/e19040141.
Smith, S.M., Fox, P.T., Miller, K.L., Glahn, D.C., Fox, P.M., Mackay, C.E., Filippini, N., Watkins, K.E., Toro, R., Laird, A.R., Beckmann, C.F., 2009. Correspondence of the brain's functional architecture during activation and rest. Proc Natl Acad Sci USA 106, 13040. doi:10.1073/pnas.0905267106.
Song, J., Birn, R.M., Boly, M., Meier, T.B., Nair, V.A., Meyerand, M.E., Prabhakaran, V., 2014. Age-related reorganizational changes in modularity and functional connectivity of human brain networks. Brain Connect 4, 662–676. doi:10.1089/brain.2014.0286.
Sporns, O., Betzel, R.F., 2016. Modular brain networks. Annu Rev Psychol 67. doi:10.1146/annurev-psych-122414-033634.
Stacey, J.E., Crook-Rumsey, M., Sumich, A., Howard, C.J., Crawford, T., Livne, K., Lenzoni, S., Badham, S., 2021. Age differences in resting state EEG and their relation to eye movements and cognitive performance. Neuropsychologia 157, 107887. doi:10.1016/j.neuropsychologia.2021.107887.
Sugiura, M., 2016. Functional neuroimaging of normal aging: declining brain, adapting brain. Ageing Res. Rev. 30, 61–72. doi:10.1016/j.arr.2016.02.006.
Tagliabue, C.F., Varesio, G., Mazza, V., 2022. Inter- and intra-hemispheric age-related remodeling in visuo-spatial working memory. front. Aging Neurosci 13, 807907. doi:10.3389/fnagi.2021.807907.
Tagliazucchi, E., von Wegner, F., Morzelewski, A., Brodbeck, V., Laufs, H., 2012. Dynamic BOLD functional connectivity in humans and its electrophysiological correlates. Front. Hum. Neurosci. 6. doi:10.3389/fnhum.2012.00339.
Tatti, E., Rossi, S., Innocenti, I., Rossi, A., Santarnecchi, E., 2016. Non-invasive brain stimulation of the aging brain: state of the art and future perspectives. Ageing Res. Rev. 29, 66–89. doi:10.1016/j.arr.2016.05.006.
Theiler, J., Eubank, S., Longtin, A., Galdrikian, B., Doyne Farmer, J., 1992. Testing for nonlinearity in time series: the method of surrogate data. Physica D: Nonlinear Phenomena 58, 77–94. doi:10.1016/0167-2789(92)90102-S.
Tibon, R., Tsvetanov, K.A., Price, D., Nesbitt, D., CAN, C., Henson, R., 2021. Transient neural network dynamics in cognitive ageing. Neurobiol. Aging 105, 217–228. doi:10.1016/j.neurobiolaging.2021.01.035.
Timme, N., Alford, W., Flecker, B., Beggs, J.M., 2014. Synergy, redundancy, and multivariate information measures: an experimentalist's perspective. J Comput Neurosci 36, 119–140. doi:10.1007/s10827-013-0458-4.
Toro, R., Fox, P.T., Paus, T., 2008. Functional coactivation map of the human brain. Cereb. Cortex 18, 2553. doi:10.1093/cercor/bhn014.
Turner, G.R., Spreng, R.N., 2012. Executive functions and neurocognitive aging: dissociable patterns of brain activity. Neurobiol. Aging 33, 826. doi:10.1016/j.neurobiolaging.2011.06.005, e1-826.e13.
Tyszka, J.M., Kennedy, D.P., Adolphs, R., Paul, L.K., 2011. Intact bilateral resting-state networks in the absence of the corpus callosum. J Neurosci 31, 15154. doi:10.1523/JNEUROSCI.1453-11.2011.
Van de Steen, F., Faes, L., Karahan, E., Songsiri, J., Valdes-Sosa, P.A., Marinazzo, D., 2019. Critical comments on EEG sensor space dynamical connectivity analysis. Brain Topogr 32, 643–654. doi:10.1007/s10548-016-0538-7.
Vlahou, E.L., Thurm, F., Kolassa, I.-.T., Schlee, W., 2014. Resting-state slow wave power, healthy aging and cognitive performance. Sci Rep 4, 5101. doi:10.1038/srep05101.
Yuval-Greenberg, S., Tomer, O., Keren, A.S., Nelken, I., Deouell, L.Y., 2008. Transient induced gamma-band response in EEG as a manifestation of miniature saccades. Neuron 58, 429–441. doi:10.1016/j.neuron.2008.03.027.
Zangrossi, A., Zanzotto, G., Lorenzoni, F., Indelicato, G., Cannas Aghedu, F., Cermelli, P., Bisiacchi, P.S., 2021. Resting-state functional brain connectivity predicts cognitive performance: an exploratory study on a time-based prospective memory task. Behav. Brain Res. 402. doi:10.1016/j.bbr.2021.113130, 113130–113130.